Since January 2020 Elsevier has created a COVID-19 resource centre with free information in English and Mandarin on the novel coronavirus COVID-19. The COVID-19 resource centre is hosted on Elsevier Connect, the company's public news and information website.

Chaos, Solitons and Fractals 141 (2020) 110364

Contents lists available at ScienceDirect

Chaos, Solitons and Fractals

Nonlinear Science, and Nonequilibrium and Complex Phenomena

journal homepage: www.elsevier.com/locate/chaos

Analyzing the impact of the media campaign and rapid testing for COVID-19 as an optimal control problem in East Java, Indonesia

Dipo Aldila

Department of Mathematics, Universitas Indonesia, Depok 16424, Indonesia

ARTICLE INFO

Article history:
Received 14 July 2020
Revised 10 October 2020
Accepted 14 October 2020
Available online 15 October 2020

2010 MSC:
34D05
92D30

Keywords:
COVID-19
Media campaign
Rapid testing
Optimal control

ABSTRACT

Without any vaccine or medical intervention to cure the infected individual from COVID-19, the non-pharmaceutical intervention become the most reasonable intervention against the spread of COVID-19. In this paper, we proposed a deterministic model governed by a system of nonlinear differential equations which consider the intervention of media campaign to increase human awareness, and rapid testing to track the undetected cases in the field. Analysis of the autonomous model shows the existence of transcritical bifurcation at a basic reproduction number equal to one. We estimate our parameter using the incidence data from East Java, Indonesia. Using these parameters, we analyze the sensitivity of the parameters in determining the size of the basic reproduction number. An optimal control problem which transforms media campaign and rapid testing as a time-dependent control was conducted also in this article. Cost-effectiveness analysis using the Infection averted ratio (IAR) and the Average cost-effectiveness ratio (ACER) conducted to analyze the best strategies to eradicate COVID-19 spread. We observe that the combination of the media campaign and rapid testing as time-dependent interventions reduces the number of an infected individual significantly and also minimizes the economic burden due to these strategies in East Java.

1. Introduction

The world has been shocked by an attack of new Coronavirus, which initially founded at the end of December 2019, which now known as COVID-19 [1]. As of July 13, 2020, total cases in all countries in the world have been reaching more than 13 million cases, with the number of deaths is about 570 thousand cases [2], and still increasing. Indonesia has the highest COVID-19 incidence in South East Asia, with a total of positive cases is about 76 thousand [2]. The first documented cases in Indonesia were recorded on March 3, 2020, in Jakarta [3]. Since then, COVID-19 spread to another province, including East Java, which now becomes one of the provinces with the highest incidence in Indonesia. As per July 13, 2020, total cases in East Java is 16 682 cases, which contribute to 22% from total cases in Indonesia [4].

Covid-19 is transmitted from human-to-human through direct contact with infected individuals or objects that had been contaminated with the viruses on the surfaces [5]. The incubation period of COVID-19 is approximately 2–14 days [6]. The symptoms of COVID-19 are varying, from fever, coughing, difficulty in breathing, and pneumonia for severe cases [7]. There is no vaccine available in the market until now, which forces the policymaker to use another intervention to suppress the spread of COVID-19, such as physical/social distancing, use of face-masks, quarantine, hospitalization, rapid testing, etc. Media campaigns have been conducted by policymakers to develop the awareness of the community to the danger of COVID-19. More aware of the community, more easy the policymaker to implement mass action to reduce the spread of COVID-19, for example, by conducting physical distancing even for the susceptible individuals, using medical masks, etc. Another popular intervention is the rapid testing which conducted to trace the undetected cases in the field and then isolating or hospitalizing them if they have been infected by COVID-19.

A mathematical model plays an important role in helping the community to understand the epidemic behavior of COVID-19, and furthermore, will help policymakers to develop a better intervention strategy to eradicate COVID-19. Various approaches have been conducted by many authors, such as with ordinary differential equations [3,8–10], fractional derivatives [11–14], artificial intelligence [15,16], and many more [17–20]. The aim of the mentioned paper is to understand the behavior of the data of COVID-19 using their proposed model, predicting the future dynamic, and proposed scenarios that might be implemented in the field to reduce the spread of COVID-19. However, only a few articles which discuss COVID-19 in Indonesia using a mathematical model. Au-

E-mail address: aldiladipo@sci.ui.ac.id

https://doi.org/10.1016/j.chaos.2020.110364
0960-0779/

thor in [3] discuss the spread of COVID-19 in Jakarta, Indonesia. Their result was suggesting massive rapid testing to compromise the relaxing of physical distancing. Another research who use incidence data in Indonesia can be seen in [10] which consider human awareness on the transmission term. The author in [21] using deterministic and stochastic models to describe the dynamic of COVID-19 in the early take-off period.

Different from the mentioned references, we are focusing this article on understanding the dynamic of COVID-19 in East Java, Indonesia. We develop a S_uS_aEAIR model, which considering two susceptible compartments to accommodate the aware and unaware subpopulation. Furthermore, rapid testing also involved in the model to trace undetected cases in the community. The infection parameters then fitted using the incidence data from East Java and used in optimal control simulations to determine the best strategies to eradicate COVID-19 in East Java.

This paper is organized as follows. We carefully construct our model in Section 2, and analyze the existence and the stability criteria of all equilibrium point, which depending on the basic reproduction number. In Section 3, the optimal control problem was characterized using the Pontryagin's Maximum Principle. Some numerical simulations regarding the parameter estimation for COVID-19 incidence data in East Java, sensitivity analysis of the basic reproduction number, autonomous simulation, and the optimal control problem were conducted in Section 4. Some conclusions are given in the last section of this article.

2. Model construction and analytical results

This section presents the new model proposed to understand the spread of COVID-19 under the effect of rapid testing and media campaign. This section contain model construction and mathematical analysis regarding the qualitative behavior of the model.

2.1. The model

The model was based on a nonlinear system of ordinary differential equations. The model takes into account the intervention by the policymaker, which promote the “self-isolation” for all individuals to avoid infection of COVID-19, and also the implementation of rapid testing to trace the undetected cases in the field.

Let us consider that the total of the human population can be separated into susceptible unaware, susceptible aware, exposed, undetected infected cases, detected infected cases, and recovered, which denoted by S_u, S_a, E, A, I, and R, respectively. We assume that the aware subpopulation conducts a health protocol to reduce the probability of getting infected by COVID-19, such as self-isolation, using medical masks, conduct physical distancing, and so on. We assume that all newborn Λ are unaware susceptible individual. Hence, we have that $\frac{dS_u}{dt} = \Lambda$. The S_u compartment then will decreasing due to infection caused by contact with I and A compartment, with the infection rate of β_1. Since A is the class for undetected individuals, we assume that the infection rate from A individual is larger than with I, which has a multiplication factor $\sigma > 1$. Hence, the number of new infection from S_u is $\beta_1 S(I + \sigma A)$. This compartment also decreases due to the effect of the media campaign by the government to avoid infection with an infected individual. This campaign is given at the rate of u_1, which will transfer S_u individual into S_a. The individuals in S_a are assumed to always conduct a careful social interaction, like using a medical mask, reducing contact by conducting a self-isolation at home, using disinfectant after touching suspicious surfaces, and many more. Hence, the infection rate for S_a is lesser than with S_u, which we denote with β_2, where $\beta_2 < \beta_1$. It is assumed that it exists a drop-out rate from S_a to S_u due to the awareness vanishing, which we denote with α.

We now describe the dynamic in the compartment of E. This compartment increases due to new infection from S_u and S_a, and decreases due to transition to be infectious individual after the incubation period of δ^{-1}. The individual from E then transferred into A and I compartment, with a proportion of p ad $1-p$, respectively. Since A compartment is the undetected case, we assume that this compartment will progress to I caused by two reasons. First is caused by the disease's progression from asymptomatic to a symptomatic individual with a rate of ξ which made this individuals volunteer to go to the hospital, and the second is caused by rapid testing intervention with the rate of u_2. We assume that only I individual who can die due to disease, with a constant rate of ϕ. Using the natural recovery rate from A and I compartment as γ_1 and γ_2, where $\gamma_2 > \gamma_1$, the dynamic of COVID-19 under the effect of the media campaign and rapid testing is given as follows.

$$\begin{aligned}
\frac{dS_u}{dt} &= \Lambda - \beta_1 S_u(I + \sigma A) - u_1 S_u + \alpha S_a - \mu S_u,\\
\frac{dS_a}{dt} &= u_1 S_u - \alpha S_a - \beta_2 S_a(I + \sigma A) - \mu S_a,\\
\frac{dE}{dt} &= (\beta_1 S_u + \beta_2 S_a)(I + \sigma A) - \delta E - \mu E,\\
\frac{dA}{dt} &= p\delta E - (\xi + u_2)A - \mu A - \gamma_1 A,\\
\frac{dI}{dt} &= (1-p)\delta E + (\xi + u_2)A - \gamma_2 I - \phi I - \mu I,\\
\frac{dR}{dt} &= \gamma_1 A + \gamma_2 I - \mu R,
\end{aligned} \tag{1}$$

where μ is the natural death rate. Please note that system (1) is supplemented with a non-negative initial condition

$$S_u(0) > 0, S_a(0) \geq 0, E(0) \geq 0, A(0) \geq 0, I(0) \geq 0, R(0) \geq 0. \tag{2}$$

All parameters are non-negative and described in Table 1.

Table 1
Definitions and value ranges for the parameters in the system (1).

Param.	Description	Value/Interval	Source
Λ	Human recruitment rate	$\frac{49\,316\,712}{70\times 365}$	Assumed
μ	Natural death rate	$\frac{1}{70\times 365}$	[22]
ϕ	Death rate induced by COVID-19	0.015	[23]
β_1	Effective contact rate of S_u	1.2644×10^{-8}	Fitted
β_2	Effective contact rate of S_a	2.253×10^{-9}	Fitted
σ	Correction factor of β for A	2	Assumption
δ	Rate due to incubation period of exposed individuals	$\frac{1}{5.1}$	[6,24–26]
p	Proportion of exposed individuals who become symptomatic individuals	0.4	[27,28]
γ_1	Recovery rate of undetected individuals	0.1	[29]
γ_2	Recovery rate of detected individuals	0.13978	[23]
ξ	Progression from asymptomatic to symptomatic individual	0.01	Assumed
α	drop out rate due to loose of awareness	0.1	Assumed
u_1	Transition rate from S_u to S_a due to media campaign	0.398	fitted
u_2	The rate of rapid testing	0.306	fitted

2.2. Basic properties of the model

The population can not be negative for all time $t \geq 0$. Hence it is crucial to show that the solution of system (1) for each variables is non-negative. The following theorem state this properties.

Theorem 1. *Any solution (S_u, S_a, E, A, I, R) of system (1) with non-negative initial conditions (2) is positive for all time $t > 0$.*

Proof. Please see Appendix A. □ □

Next, we analyze how the solution of system (1) is bounded. The following theorem confirm this properties.

Theorem 2. *The solution of (S_u, S_a, E, A, I, R) of system (1) is bounded in the region*

$$\Omega = \left\{ (S_u, S_a, E, A, I, R) \in \mathbb{R}^6_+ : S_u + S_a + E + A + I + R \leq \frac{\Lambda}{\mu} \right\}. \quad (3)$$

Proof. Please see Appendix B. □ □

2.3. Analytical results on the equilibrium and the basic reproduction number

System (1) always had a trivial COVID-19 free equilibrium which given by

$$E_0 = (S_u, S_a, E, A, I, R) = \left(\frac{\Lambda(\alpha+\mu)}{\mu(\alpha+\mu+u_1)}, \frac{\Lambda u_1}{\mu(\alpha+\mu+u_1)}, 0, 0, 0, 0 \right), \quad (4)$$

and the basic reproduction number is given by (See Appendix C for the derivation of $\mathscr{R}_0$)

$$\mathscr{R}_0 = \mathscr{R}_{\text{undetected}} + \mathscr{R}_{\text{detected-1}} + \mathscr{R}_{\text{detected-2}}, \quad (5)$$

where

$$\mathscr{R}_{\text{undetected}} = \frac{\sigma\,\Lambda\,(\beta_1\alpha + \beta_1\mu + u_1\beta_2)\delta\, p}{\mu\,(\alpha+\mu+u_1)(\mu+\xi+\gamma_1+u_2)(\delta+\mu)}, \quad (6)$$

$$\mathscr{R}_{\text{detected-1}} = \frac{\Lambda\,(\alpha\,\beta_1 + \beta_1\mu + u_1\beta_2)\delta\,(\mu+\gamma_1)(1-p)}{\mu\,(\mu+\xi+\gamma_1+u_2)(\gamma_2+\mu+\phi)(\delta+\mu)(\alpha+\mu+u_1)}, \quad (7)$$

$$\mathscr{R}_{\text{detected-2}} = \frac{\Lambda\,(\alpha\,\beta_1 + \beta_1\mu + u_1\beta_2)\delta\,(\xi+u_2)}{\mu\,(\mu+\xi+\gamma_1+u_2)(\gamma_2+\mu+\phi)(\delta+\mu)(\alpha+\mu+u_1)}. \quad (8)$$

It can be seen that $\mathscr{R}_0$ in (5) were constructed by three component. The first component is $\mathscr{R}_{\text{undetected}}$ which describe the infection in S_u and S_a due to contact with undetected individuals. The $\mathscr{R}_{\text{detected-1}}$ describe an infection from detected individual which directly coming from the path of $E \to I$, while $\mathscr{R}_{\text{detected-2}}$ is coming from the path of $E \to A \to I$. Since the infection rate from undetected individual is larger than from detected individual ($\sigma > 1$), increasing u_2 will reduce $\mathscr{R}_{\text{detected-2}}$. Furthermore, it also can be seen that increasing u_1 will reduce $\mathscr{R}_0$.

Using Theorem 2 in [31], an important results regarding local stability of E_0 stated as follows.

Theorem 3. *COVID-19 model in (1) is locally asymptotically stable if $\mathscr{R}_0 < 1$, and unstable when $\mathscr{R}_0 > 1$.*

This theorem has been reviewed by the author in [31]. Hence, we do not show it in this article. The theorem implies that it is possible to eradicate COVID-19 if this threshold is less than unity. The basic reproduction number is defined as an expected number of secondary cases due to infection from one primary case during its infection period in a completely susceptible population [32]. Many epidemiological models generate the same results (see [33–35] for some examples). However, not always $\mathscr{R}_0 < 1$ indicates the disease may not persist. When backward bifurcation appears, another stable equilibrium, which in this case is the endemic equilibrium, is locally stable. Please refer to [3,36–38] for examples. Hence, it is important to understand the bifurcation type of our proposed model in (1).

The next equilibrium is the endemic equilibrium, which is given as follows.

$$E_1 = (S_u, S_a, E, A, I, R) = \left(S_u^\dagger, S_a^\dagger, E^\dagger, A^\dagger, I^\dagger, R^\dagger\right) \quad (9)$$

where

$$S_u^\dagger = \frac{\Lambda(A^\dagger\sigma\,\beta_2 + \alpha + \mu)}{\left(A^\dagger\sigma\,\beta_2 + \alpha + \mu\right)\left(A^\dagger\sigma + In^\dagger\right)\beta_1 + A^\dagger\mu\,\sigma\,\beta_2 + A^\dagger\sigma\,\beta_2 u_1 + In^\dagger\alpha\,\beta_2 + \alpha\,\mu + \mu^2 + \mu\,u_1},$$

$$S_a^\dagger = \frac{\Lambda(u_1 - \beta_2 I^\dagger)}{\left(A^\dagger\sigma\,\beta_2 + \alpha + \mu\right)\left(A^\dagger\sigma + In^\dagger\right)\beta_1 + A^\dagger\mu\,\sigma\,\beta_2 + A^\dagger\sigma\,\beta_2 u_1 + In^\dagger\alpha\,\beta_2 + \alpha\,\mu + \mu^2 + \mu\,u_1},$$

$$E^\dagger = \frac{pA^\dagger(\mu+\xi+\gamma_1+u_2)}{\delta p},$$

$$I^\dagger = \frac{((1-p)(\gamma_1+\mu)+\xi+u_2)A^\dagger}{p(\phi+\gamma_2+\mu)},$$

$$R^\dagger = \frac{A^\dagger(p\gamma_1(\mu+\phi)+(1-p)\mu\gamma_2+\xi\,\gamma_2+\gamma_1\gamma_2+\gamma_2 u_2)}{p\mu\,(\gamma_2+\mu+\phi)}.$$

$A\dagger$ is taken from the positive roots of the following polynomial

$$\mathscr{P}(A) = a_2A^2 + a_1A + a_0 = 0, \quad (10)$$

where

$$\begin{aligned}
a_2 &= -\beta_1\beta_2(\mu+\xi+\gamma_1+u_2)(\mu\,p\sigma + p\phi\,\sigma + p\sigma\,\gamma_2 \\
&\quad +(1-p)(\mu+\gamma_1)+\xi+u_2)^2(\delta+\mu), \\
a_1 &= p\delta\beta_1\beta_2\Lambda(\mu\,p\sigma + p\phi\,\sigma + p\sigma\,\gamma_2 + (1-p)(\mu+\gamma_1) \\
&\quad +\xi+u_2)^2\cdots - p(\mu\,p\sigma + p\phi\,\sigma + p\sigma\,\gamma_2 + (1-p)(\mu+\gamma_1) \\
&\quad +\xi+u_2)(\mu+\xi+\gamma_1+u_2)\ldots \\
&\quad (\gamma_2+\mu+\phi)\,(\delta+\mu)\,(\beta_1(\alpha+\mu)+\beta_2(\mu+u_1), \\
a_0 &= p^2(\gamma_2+\mu+\phi)\mu\,(\alpha+\mu+u_1)(\mu+\xi+\gamma_1+u_2)(\delta+\mu)(\mathscr{R}_0-1).
\end{aligned}$$

From the expression of $\mathscr{P}(A)$, it can be seen that a_2 always negative, while $a_0 > 0 \iff \mathscr{R}_0 > 1$. Hence, we have the following theorem regarding the existence of the endemic equilibrium when $\mathscr{R}_0 > 1$.

Theorem 4. *COVID-19 model in (1) is always has a unique COVID-19 endemic equilibrium given by (9) whenever $\mathscr{R}_0 > 1$.*

Since $\mathscr{P}(A)$ is a two degree polynomial, we have a possibility to have two COVID-19 endemic equilibrium when $\mathscr{R}_0 < 1$. $\mathscr{P}(A)$ have

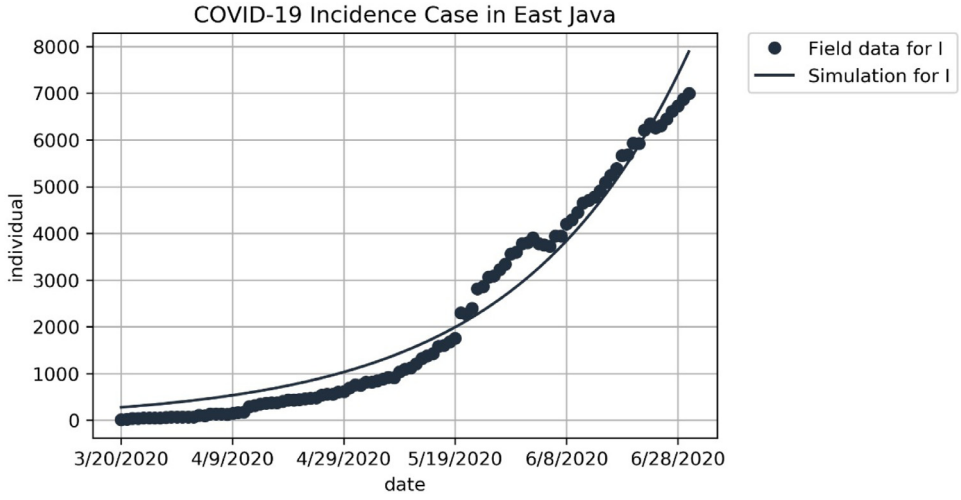

(a)

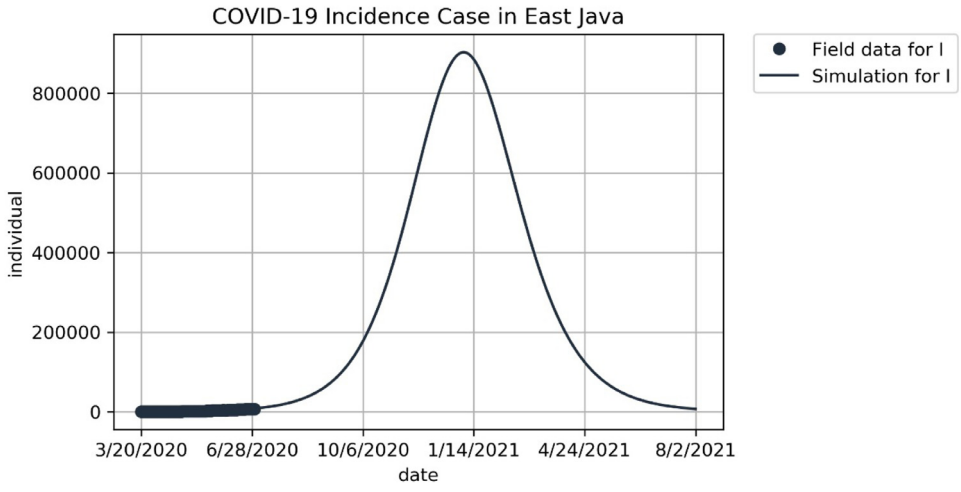

(b)

Fig. 1. Time series plot showing the performance of least square method for system (1) for East Java in a short-period (a), and long period (b). The black dots represent the incidence data, and the solid lines represent the prediction of total infected cases.

two positive roots if $a_0 > 0 \iff \mathscr{R}_0 > 1$, $a_1 < 0$ and $a_1^2 - 4a_2a_0 > 0$. However, this condition never fulfilled, which we state in the following lemma.

Lemma 1. *Polynomial $\mathscr{P}(A)$ never has a positive roots when $\mathscr{R}_0 < 1$.*

Proof. Please see Appendix D for the proof. □

Since we always have a stable COVID-19 free equilibrium without any exist COVID-19 endemic equilibrium when $\mathscr{R}_0 < 1$, and it always exist a unique COVID-19 endemic equilibrium when $\mathscr{R}_0 > 1$, our system (1) indicate a transcritical bifurcation occurrence at $\mathscr{R}_0 = 1$.

3. Numerical experiments

3.1. Parameter estimation

To conduct a simulation in this article, we use parameters value as shown in Table 1, while the effective contact rate β_1 and β_2, and the media campaign rate u_1 and rapid testing rate u_2 were estimated from incidence data. The incidence data of East Java are taken from [4] from Mei 20 to June 30, 2020. Total of population in East Java is 49 316 712. The result of parameter estimation is shown in Fig. 1 with the best fit parameter is $\beta_1 = 1.2644 \times 10^{-8}$, $\beta_2 = 2.253 \times 10^{-9}$, $u_1 = 0.398$, and $u_2 = 0.306$. With this parameter values, the basic reproduction number in East Java is 1.66 which indicates the existence of the endemic equilibrium of COVID-19. The endemic equilibrium is given by

$$E_1 = (S_u, S_a, E, A, I, R) = \left(5.96 \times 10^6, 2.37 \times 10^7, 4\,217,795, 4\,827, 1.789 \times 10^7\right).$$

3.2. Discussion on the effect of constant control on $\mathscr{R}_0$ and the autonomous system

From the previous analysis, we can see that the basic reproduction number determines the qualitative behavior of our COVID-19 model. Hence, it is important to analyze the most significant parameter that can change the value of $\mathscr{R}_0$. To conduct this, we use the local sensitivity analysis respect to $\mathscr{R}_0$ using the best-fitted parameter for East Java incidence data.

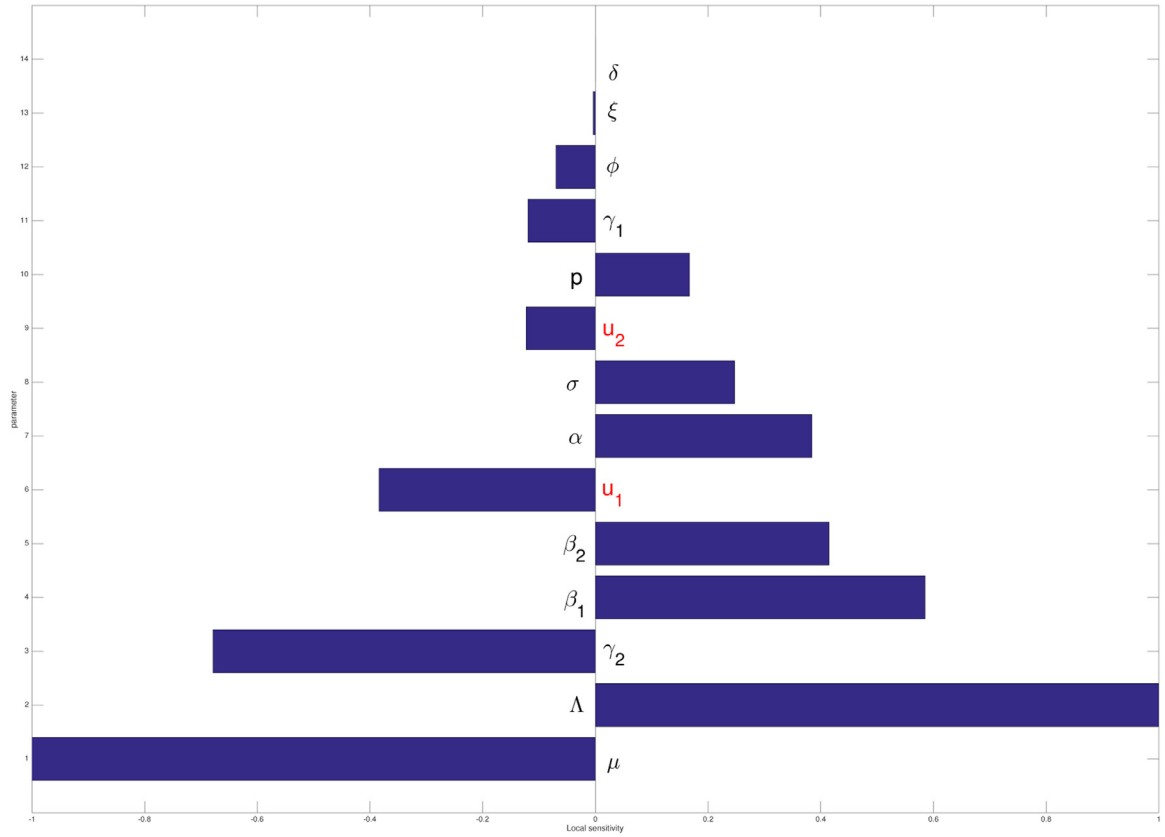

Fig. 2. Local sensitivity analysis of $\mathscr{R}_0$.

Definition 1. (See [39]). The normalized forward sensitivity index of $\mathcal{R}_0$, with respect to a given parameter θ, is defined by

$$\mathcal{E}_{\theta}^{\mathcal{R}_0} = \frac{\partial \mathcal{R}_0}{\partial \theta} \times \frac{\theta}{\mathcal{R}_0}.$$

Since $\frac{\partial \mathscr{R}_0}{\partial \beta_1} = \frac{\delta\,(\mu\, p\sigma + p\phi\,\sigma + p\sigma\,\gamma_2 - p\mu - \gamma_1 p + \mu + \xi + \gamma_1 + u_2)(\alpha+\mu)\Lambda}{\mu\,(\mu+\xi+\gamma_1+u_2)(\gamma_2+\mu+\phi)(\delta+\mu)(\alpha+\mu+u_1)}$, then we have that

$$\mathcal{E}_{\beta_1}^{\mathcal{R}_0} = \frac{\partial \mathcal{R}_0}{\partial \beta_1} \times \frac{\beta_1}{\mathcal{R}_0} = \frac{(\alpha+\mu)\beta_1}{\alpha\,\beta_1 + \beta_1\mu + u_1\beta_2}.$$

Substituting parameter values on Table 1, we have that $\mathcal{E}_{\beta_1}^{\mathcal{R}_0} = 0.5851$. This means that increasing β_1 for 10% will increase $\mathscr{R}_0$ for 5.851%. We calculate the local sensitivity of all parameters value in $\mathscr{R}_0$ in a similar way with β_1, and the result is given in Fig. 2. We can see that the most significant parameter in $\mathscr{R}_0$ is μ, followed with Λ, Γ_2, β_1, β_2, u_1, α, σ, u_2, p, γ_1, ϕ, ξ, and δ, respectively. This results indicates that u_1 is more sensitive than u_2 in determining $\mathscr{R}_0$.

Based on Theorem 4 and 6, we notice that $\mathscr{R}_0$ holds an important role in determining the existence and type of stability of each equilibrium points. We have that COVID-19 dies out whenever $\mathscr{R}_0 < 1$, and exist whenever $\mathscr{R}_0 > 1$. Hence, it is important to reduce the magnitude of $\mathscr{R}_0$ as small as possible until it is less than one. Since

$$\frac{\partial \mathscr{R}_0}{\partial u_1} = -\frac{\delta\,(\mu\, p\sigma + p\phi\,\sigma + p\sigma\,\gamma_2 + (1-p)(\mu+\gamma_1) + \xi + u_2)\Lambda\,(\beta_1 - \beta_2)(\alpha+\mu)}{\mu\,(\mu+\xi+\gamma_1+u_2)(\gamma_2+\mu+\phi)(\delta+\mu)(\alpha+\mu+u_1)^2} < 0,$$

and

$$\frac{\partial \mathscr{R}_0}{\partial u_2} = -\frac{\delta\,\Lambda\,(\alpha\,\beta_1 + \beta_1\mu + u_1\beta_2)p(\mu(\sigma-1) + \phi\,\sigma + \sigma\,\gamma_2 - \gamma_1)}{\mu\,(\mu+\xi+\gamma_1+u_2)^2(\gamma_2+\mu+\phi)(\delta+\mu)(\alpha+\mu+u_1)} < 0,$$

we can conclude that increasing the implementation of the media campaign and rapid testing will reduce the chance of COVID-19 to exist in the population. Increasing the media campaign for 10% will reduce $\mathscr{R}_0$ 3.843%. On the other hand, increasing the rapid testing rate for 10% will reduce $\mathscr{R}_0$ for 1.23%. Using parameters value as shown in Table 1, the contour plot of u_1 and u_2 respect to $\mathscr{R}_0$ is given in Fig. 3. It can be seen that u_1 and u_2 is inversely proportional to $\mathscr{R}_0$. It means that increasing media campaigns and/or rapid testing will increase the chance to eradicate COVID-19 from the community.

The sensitivity of $\mathscr{R}_0$ respect to u_1 and u_2 when β_2 is varying is given in Fig. 4. We conduct the sensitivity of u_1 and u_2 by reducing β_2 75%, 80%, 85%, 90%, and 95%. It can be seen that larger the value of β_2 will requires more intense of media campaign and rapid test that should be implemented to achieve a condition of COVID-19 free equilibrium.

From all sensitivity analysis that had been conducted in Figs. 2–4, we can see that there is a big chance to eradicate COVID-19 from East Java, where using the media campaign could give better result rather than only depending on rapid testing. Increasing community awareness through a media campaign in our model will reduce the infection rate of the aware population. This can be done when this aware population is encouraged to do a physical distancing, using medical masks, and any other intervention which in our model will reduce the value of β_2.

Next, we simulate our proposed COVID-19 model in (1) using parameters value in Table 1, except it stated differently, to assess the impact of various possible control strategies against COVID-19 in East Java. First, we simulate the impact of the media campaign

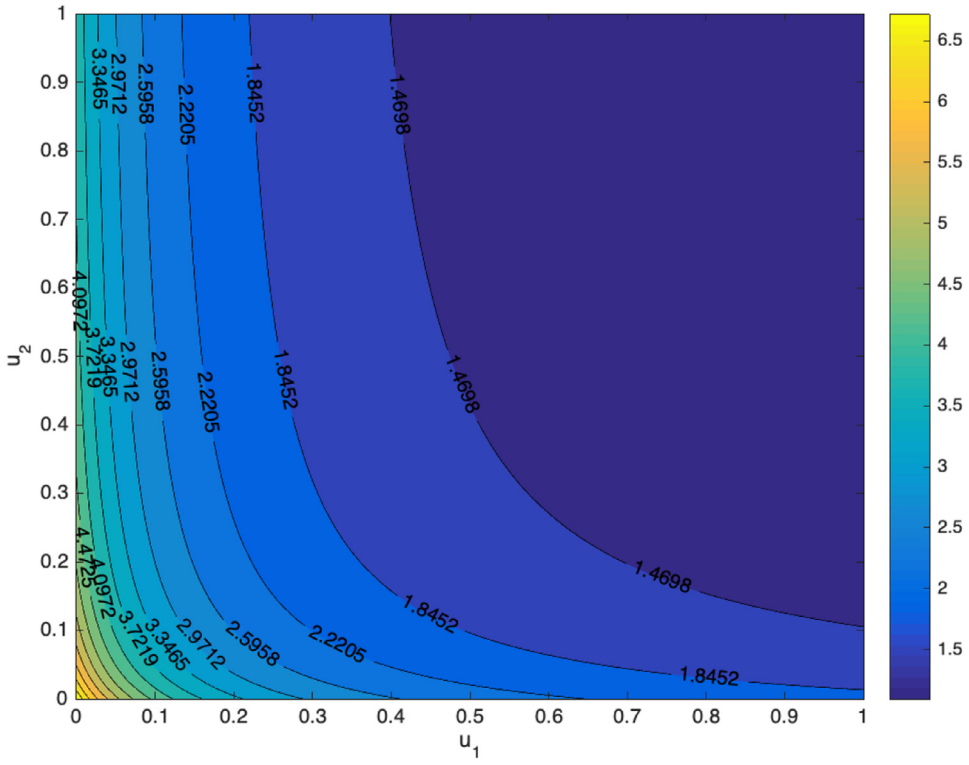

Fig. 3. Contour plot of the basic reproduction number respect to media campaign u_1 and rapid testing u_2.

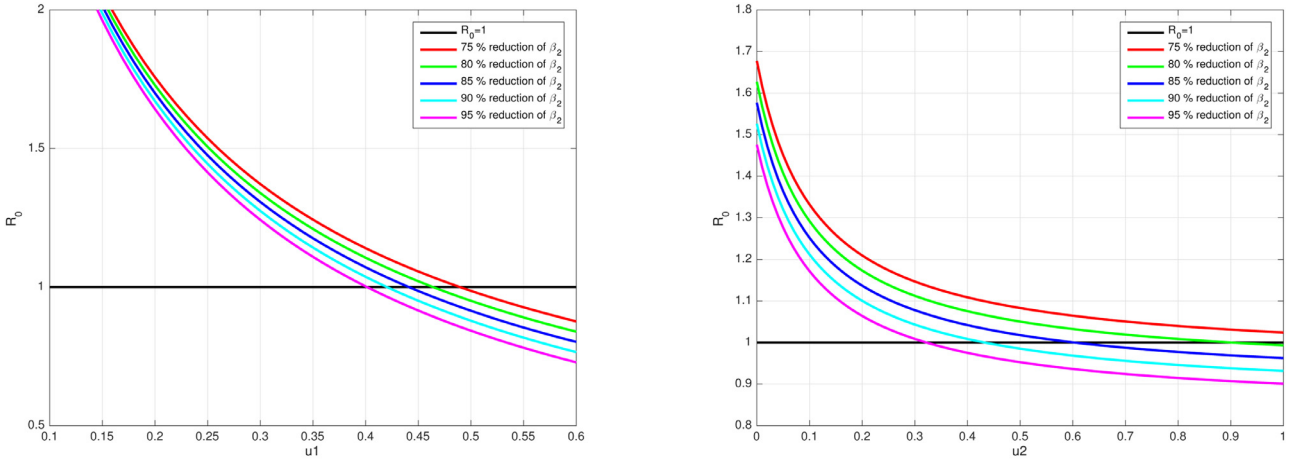

Fig. 4. Profile of the reproduction number as a function of u_1 (a) and u_2 (b) respect to the change of β_2.

by the government to increase the number of aware population. Hence, we use 5 different value for u_1, where $u_1 = 0.398$ as the baseline value, while the other four values are 10%, 20%, 30%, and 40% increased. The results are given in Fig. 5. It can be seen that intervention of media campaign show a dramatic decrease in the number of infected individuals in East Java.

Second autonomous simulation is conducted to see the impact of rapid testing against the spread of COVID-19 in East Java. We set all parameters value similar to the baseline parameter used in the previous simulation, except we use five different values of u_2. The baseline value of u_2 is 0.306, while the other values are increased 10%, 20%, 30%, and 40%. The results are given in Fig. 6. Our simulation indicates how rapid testing could suppress the outbreak of COVID-19 in East Java, even though not dramatic as the implementation of a massive media campaign. This is because u_1 is more sensitive to $\mathscr{R}_0$ rather than u_2, as already explained in Fig. 2.

A simulation was further to see the impact of the media campaign's effectiveness to reduce the infection rate of the aware population. To conduct this simulation, we use the same parameter values as in the previous simulation, while β_2 will be varying for five values. The first value is 2.253×10^{-9}, while the other four values are reduced for 10%, 20%, 30%, and 40%. The result is given in Fig. 7. It can be seen that reducing the value of β_2 success to reduce the infected population massively. The result of this simulation shows how the peak of the outbreak reduced significantly, and the time for the occurrence of the outbreak also delayed.

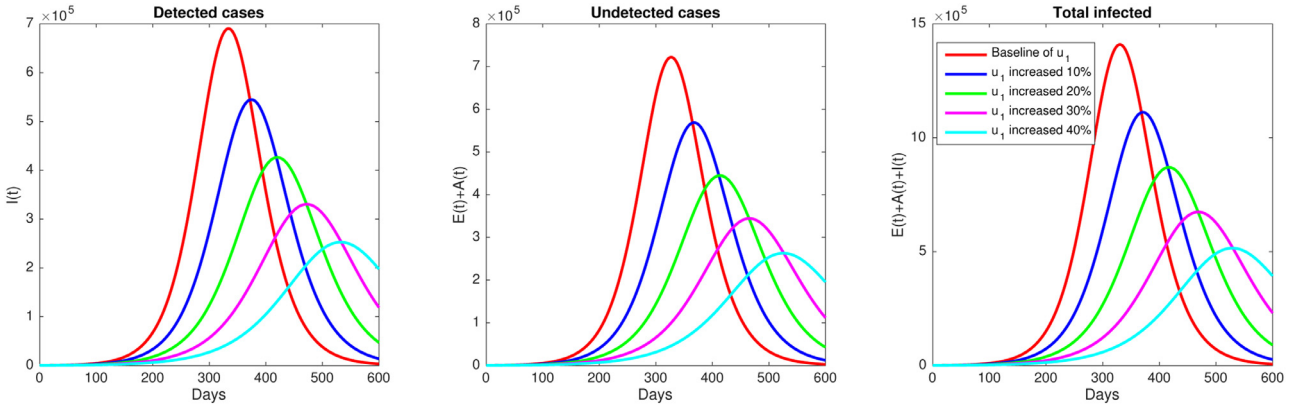

Fig. 5. Effect of media campaign (u_1). Simulation of the model (1) shows how number of infected individuals decreases when media campaign rate increasing.

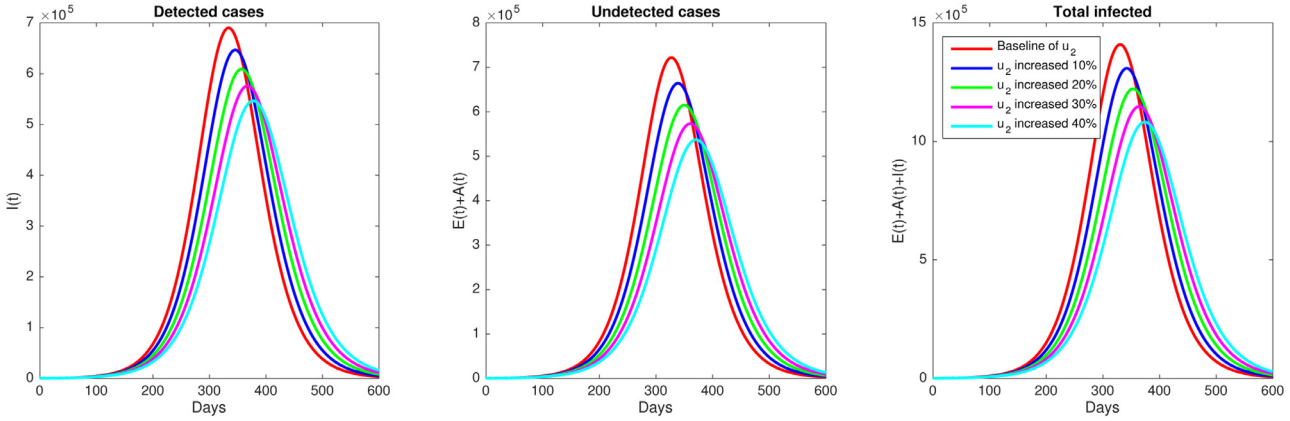

Fig. 6. Effect of rapid testing (u_2). Simulation of the model (1) shows how number of infected individuals decreases when rapid testing rate increasing.

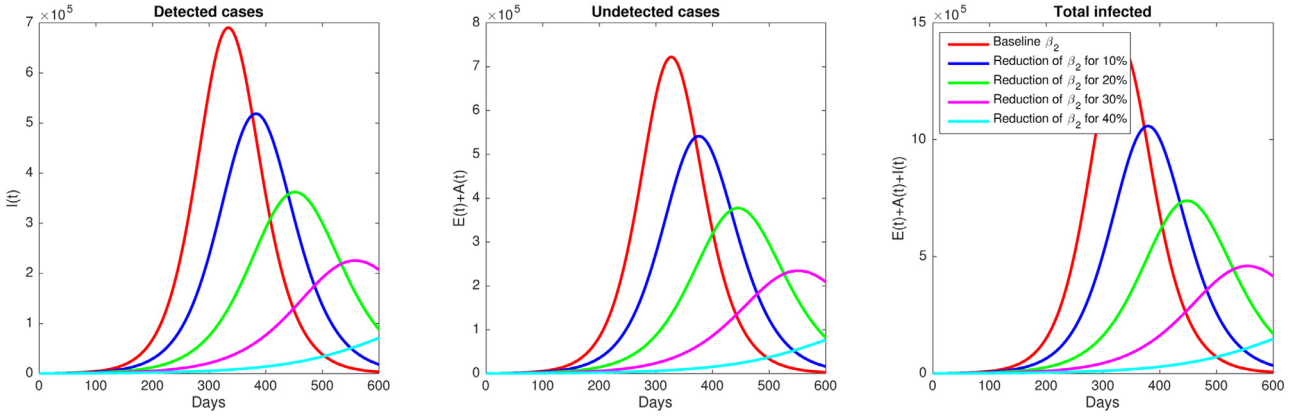

Fig. 7. Effect of reducing β_2. Simulation of the model (1) shows how number of infected individuals decreases when aware population increases their awareness to reduce the infection rate.

4. Optimal control problem

4.1. Optimal control characterization

We seek to minimize the number of infected individual E, A, and I in COVID-19 model (1) and the cost for applying media campaign u_1 and rapid testing u_2 controls. Hence, we consider our control parameters to be dependent on time, $u_1 = u_1(t)$ and $u_2 = u_2(t)$. Therefore, we have model (1) now becomes

$$\begin{aligned}
\frac{dS_u}{dt} &= \Lambda - \beta_1 S_u(I+\sigma A) - u_1(t)S_u + \alpha S_a - \mu S_u,\\
\frac{dS_a}{dt} &= u_1(t)S_u - \alpha S_a - \beta_2 S_a(I+\sigma A) - \mu S_a,\\
\frac{dE}{dt} &= (\beta_1 S_u + \beta_2 S_a)(I+\sigma A) - \delta E - \mu E,\\
\frac{dA}{dt} &= p\delta E - (\xi + u_2(t))A - \mu A - \gamma_1 A,\\
\frac{dI}{dt} &= (1-p)\delta E + (\xi + u_2(t))A - \gamma_2 I - \phi I - \mu I,\\
\frac{dR}{dt} &= \gamma_1 A + \gamma_2 I - \mu R.
\end{aligned} \tag{11}$$

We consider the objective function that describe our aim previously in the following function.

$$\mathscr{J}(u_1,u_2)=\int_0^{t_f}\left(E+A+I+\frac{c_1}{2}u_1^2+\frac{c_2}{2}u_2^2\right)dt, \tag{12}$$

where c_1 and c_2 is the weight parameters for media campaign and rapid testing, respectively, and t_f is the final time of the simulation. We assume that the cost for media campaign and rapid testing is nonlinear, hence we choose it as a quadratic function. Please see [40–44] for another examples for an implementation of a quadratic cost function in an optimal control problem for epidemiological models. The term of $\int_0^{t_f}(E+A+I)\,dt$ describe the cost related to a consequences of a high number of infected individual, for an example cost due to economic condition during pandemic. On the other hand, $\int_0^{t_f}\left(\frac{c_1}{2}u_1^2+\frac{c_2}{2}u_2^2\right)dt$, represent the cost for control implementation. Our task is to seek an optimal control trajectories of u_1^* and u_2^* such that

$$\mathscr{J}(u_1^*,u_2^*)=\min_{\Gamma}\mathscr{J}(u_1,u_2), \tag{13}$$

where Γ is the set of admissible control

$$\Gamma=\left\{(u_1,u_2)\in(L^\infty(0,t_f))^2|0\le u_i(t)\le 1 \text{ for } i=1,2\right\}.$$

Before we characterize the optimal control problem, we show the existence of such optimal control function which fulfilled above task. For this purposes, we follow the results given in [45,46].

Theorem 5. *There exists an optimal control pair u_1^* and u_2^* in Γ such that $\mathscr{J}(u_1^*,u_2^*)=\min_\Gamma\mathscr{J}(u_1,u_2)$, which correspond to COVID-19 model in (11).*

Proof. Please see Appendix E for the proof. □

The Pontryagin's Maximum principle [49] provides the necessary condition for the existence of the optimal control pair (u_1^*,u_2^*) of the model (11). The idea of this method is to convert the state system (11) and the cost function (12) with (13) into a problem of minimizing the Hamiltonian $\mathscr{H}$ with respect to u_1 and u_2 as follows

$$\begin{aligned}\mathscr{H}=&E+A+I+\frac{c_1}{2}u_1^2+\frac{c_2}{2}u_2^2+\lambda_1\frac{dS_u}{dt}+\lambda_2\frac{dS_a}{dt}+\lambda_3\frac{dE}{dt}\\&+\lambda_4\frac{dA}{dt}+\lambda_5\frac{dI}{dt}+\lambda_6\frac{dR}{dt},\end{aligned} \tag{14}$$

where λ_i for $i=1,2,3,4,5,6$ is the adjoint variables respect to S_u, S_a, E, A, I, and R, respectively. The necessary conditions for the existence of these adjoint variables and the control characterizations is given in the following theorem.

Theorem 6. *Given an optimal control pairs (u_1^*,u_2^*)which minimize the cost function (12) over Γ subject to the state system (11), then there exist an adjoint variables λ_i for $i=1,2,\ldots,6$ satisfying the following system*

$$\begin{aligned}\frac{d\lambda_1}{dt}&=\beta_1(I+\sigma A)(\lambda_1-\lambda_3)+u_1(\lambda_1-\lambda_2)+\mu\lambda_1,\\
\frac{d\lambda_2}{dt}&=\alpha(\lambda_2-\lambda_1)+\beta_2(I+\sigma A)(\lambda_2-\lambda_3)+\mu\lambda_2\\
\frac{d\lambda_3}{dt}&=-1+p\delta(\lambda_3-\lambda_4)+(1-p)\delta(\lambda_3-\lambda_5)+\mu\lambda_3,\\
\frac{d\lambda_4}{dt}&=-1+\sigma\beta_1S_u(\lambda_1-\lambda_3)+\sigma\beta_2S_a(\lambda_2-\lambda_3)\\&\quad+(\xi+u_2)(\lambda_4-\lambda_5)+\gamma_1(\lambda_4-\lambda_6)+\mu\lambda_4,\\
\frac{d\lambda_5}{dt}&=-1+\beta_1S_u(\lambda_1-\lambda_3)+\beta_2S_a(\lambda_2-\lambda_3)+\gamma_2(\lambda_5-\lambda_6)\\&\quad+(\mu+\phi)\lambda_5,\\
\frac{d\lambda_6}{dt}&=\mu\lambda_6.\end{aligned} \tag{15}$$

with a transversality condition $\lambda_i(t_f)=0$ for $i=1,2,\ldots,6$, and

$$\begin{aligned}u_1^*&=\max\left\{0,\min\left\{1,\frac{S_u(\lambda_1-\lambda_2)}{c_1}\right\}\right\},\\
u_2^*&=\max\left\{0,\min\left\{1,\frac{A(\lambda_4-\lambda_5)}{c_2}\right\}\right\}.\end{aligned} \tag{16}$$

Proof. Please see Appendix F for the proof. □

4.2. Simulation for the optimal control problem

In this section, we shall conduct a numerical simulation for the optimal control problem which already discussed in previous section. For this purposes, we define the following three strategies : **(1)** Execution only with media campaign $(u_1(t)\ge 0,u_2(t)=0)$, **(2)** Implementation of rapid testing only $(u_1(t)=0,u_2(t)\ge 0)$, and **(3)** Implementation of both intervention $(u_1(t)\ge 0,\ u_2(t)\ge 0)$.

For numerical implementation, we solve the optimality system (11) and (15) together with the control characterization (16) using numerical iterative scheme. We use the forward-backward sweep method to solve our problem. The algorithm start with an initial guess for control variable, and solve the state system (11) forward in time. After that, we solve the adjoint system (15) backward in time. Both this numerical calculation are using ode45 in MATLAB. Then, the optimal control (16) should be updated using these state and adjoint variables. This process repeated until a convergence criteria is met (see [50] for detail, and [34,35,43] for some examples). For our numerical experiments, we consider a set of parameter given in Table 1 and the time period for simulations is 100 days along with the initial condition $S_u(0)=7\,924\,040, S_a(0)=31\,517\,500, E=8\,557, A=1\,496, R=38\,071$ which is the final state of curve fitting of model (1) in Fig. 1. We choose the positive weight constant $c_1=3\times10^7$ and $c_2=3\times10^5$.

For the first scenario, when we only execute the media campaign as a single intervention, the corresponding results obtained are plotted in Fig. 8. We noticed that the media campaign should be given at a high rate from the beginning of the simulation, remain constant at around $u=0.16$ for a long time period, and start to decrease when the time is getting closer to the final time of the simulation. As a consequence of the high rate of the media campaign, the number of infected can be suppressed for a long time, but it starts to increase when the media campaign starts to decrease.

The results corresponding to strategy two $(u_1=0,u_2\ge 0)$ are shown in Fig. 9. We observed that the implementation of rapid testing is always larger than the implementation of u_1 only in the first scenario. The control trajectories of u_2 are almost always should be given at its highest rate $(u_2=1)$ and then start to decrease when it is approaching the final time of the simulation. As a result, the reduction of infected cases achieved, even though not as good as in the first scenario.

The last simulation conducted for the third scenario, when all controls executed. The results obtained in Fig. 10. One can easily see from Fig. 10 is that the infective population can be suppressed during the simulation period. As a consequence of both interventions should be executed, it can be seen that the rate of rapid testing should be reduced as a compromise for the implementation of the media campaign.

4.3. Cost-effectiveness analysis

Arising from optimal control simulation in the previous section, we need to determine the best strategy, which in this case, is the

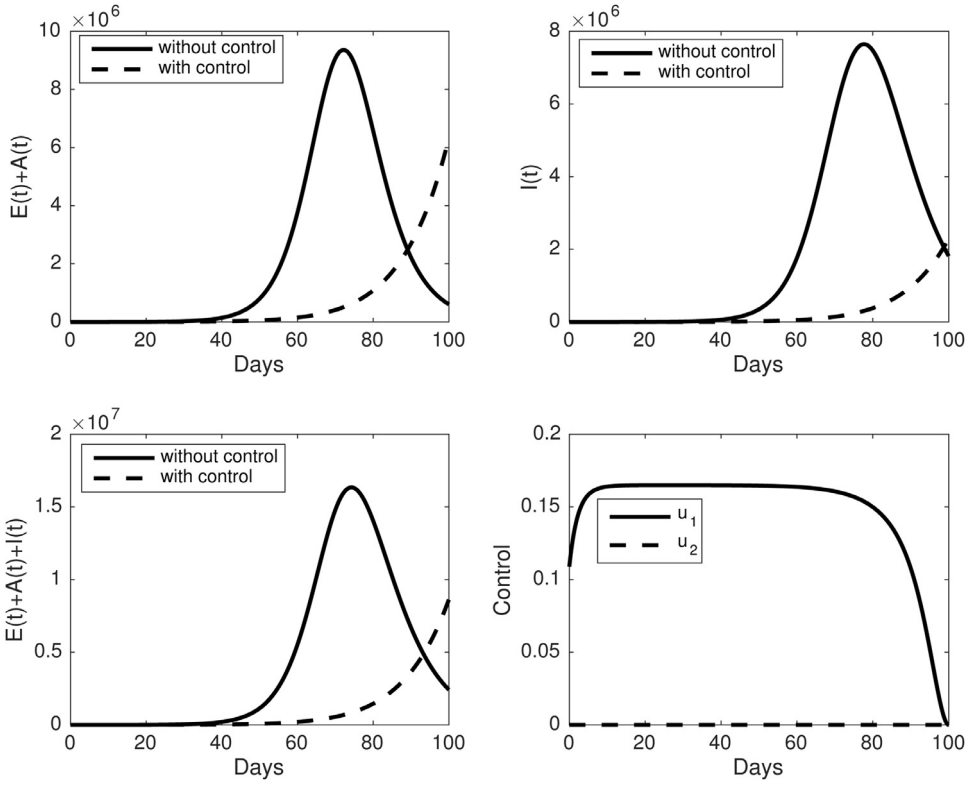

Fig. 8. The dynamic of infected individuals and control trajectories for the first scenario ($u_1 \geq 0, u_2 = 0$). Upper panel : (left) dynamic of $E(t) + A(t)$ and (right) $I(t)$. The lower panel : (left) dynamic of $E(t) + A(t) + I(t)$ and (right) control trajectories.

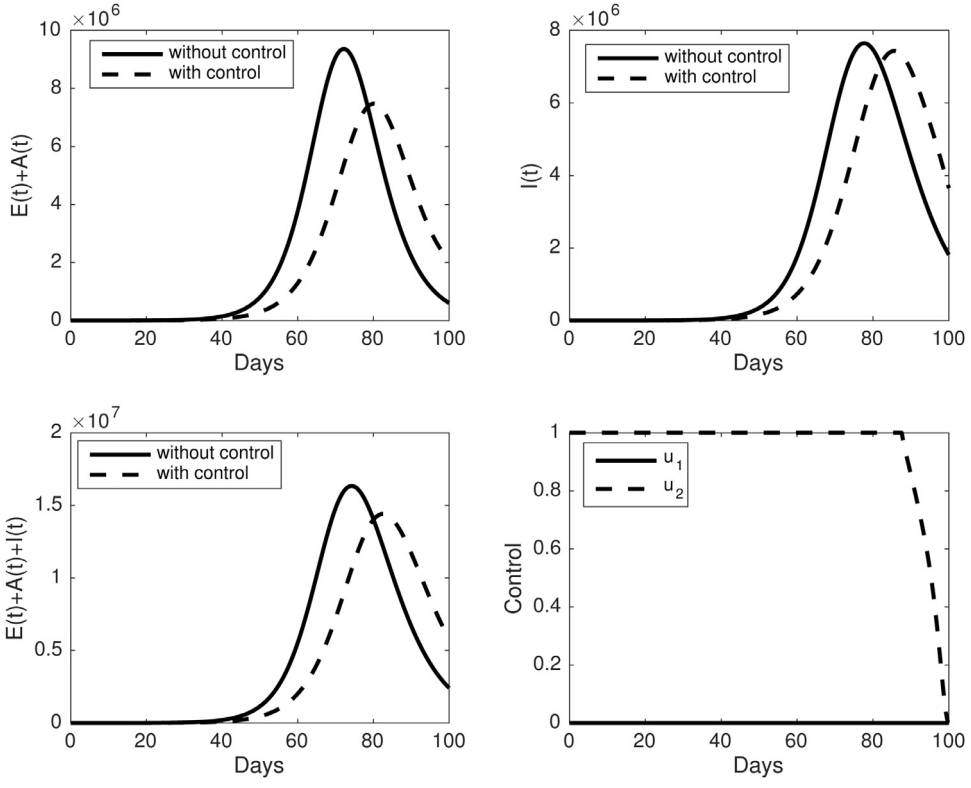

Fig. 9. The dynamic of infected individuals and control trajectories for the second scenario ($u_1 = 0, u_2 \geq 0$). Upper panel : (left) dynamic of $E(t) + A(t)$ and (right) $I(t)$. The lower panel : (left) dynamic of $E(t) + A(t) + I(t)$ and (right) control trajectories.

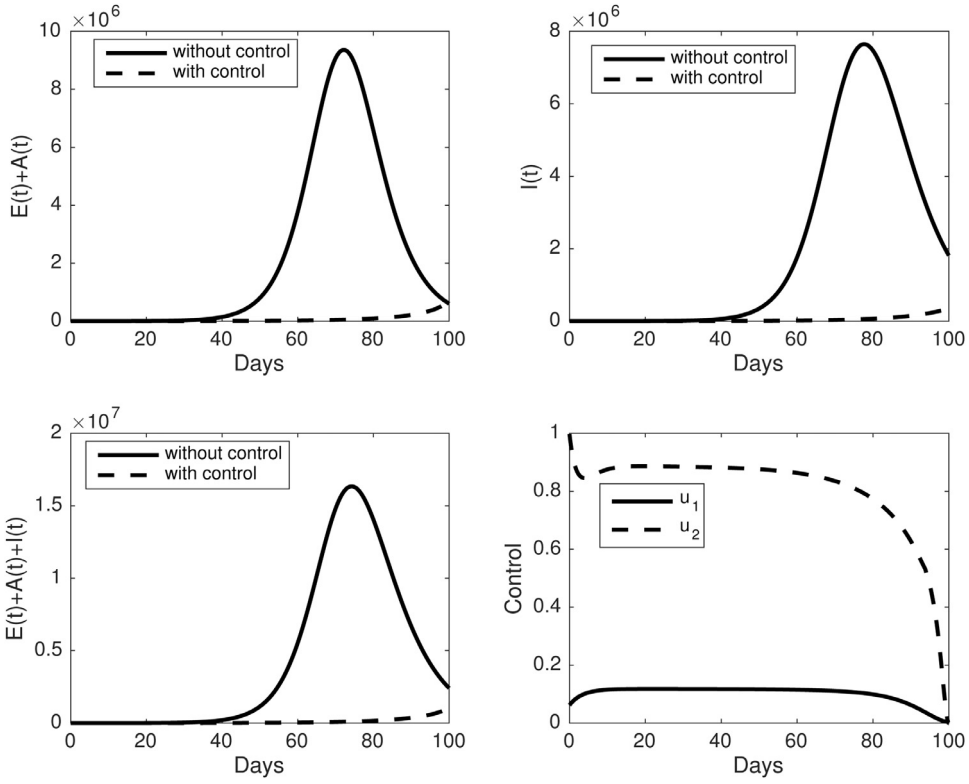

Fig. 10. The dynamic of infected individuals and control trajectories for the third scenario ($u_1 \geq 0$, $u_2 \geq 0$). Upper panel : (left) dynamic of $E(t) + A(t)$ and (right) $I(t)$. The lower panel : (left) dynamic of $E(t) + A(t) + I(t)$ and (right) control trajectories.

Table 2
Numerical results for each prevention scenario.

Strategy	Scenario	$\int_0^T (\frac{c_1}{2}u_1^2 + \frac{c_2}{2}u^2)\,dt$	$\mathcal{A}^{inf}$	IAR	ACER
1	$u_1 \geq 0, u_2 = 0$	1.159×10^8	3.417×10^8	1.69×10^3	0.339
2	$u_1 = 0, u_2 \geq 0$	2.77×10^7	5.03×10^7	3.53×10^2	0.552
3	$u_1 \geq 0, u_2 \geq 0$	6.113×10^7	4.198×10^8	3.305×10^4	0.145

most cost-effective intervention strategy to eradicate COVID-19. To do this, we conduct two cost-effectiveness analysis, namely the IAR (Infected Averted Ratio) and the ACER (Average Cost-Effectiveness Analysis). The IAR formula is given by

$$\text{IAR} = \frac{\text{Total number of infections averted}}{\text{Total number of recovered}}, \tag{17}$$

where the total number of infections averted is given by

$$\mathcal{A}^{inf} = \int_0^T (E(t) - E^*(t)) + (A(t) - A^*(t)) + (I(t) - I^*(t))\,dt, \tag{18}$$

where E^*, A^*, and I^* denote the numbers of exposed, undetected cases and detected cases individuals due to control strategies. The strategy exhibiting the highest IAR is considered to be the most effective strategy. The results for the control scenario in the previous section are given in Table 2. From Table 2, it can be seen that strategy-3 is the most effective strategy, followed with strategy-1 and strategy-2, respectively. These results show that to minimize the number of an infected individuals, the best strategy that should be considered ia the implementation of the massive media campaign and rapid testing. However, if the policymaker should choose a single intervention that should be implemented, then the media campaign is the better option rather than rapid testing.

The second cost-effectiveness analysis is the ACER with the formula as follows.

$$\text{ACER} = \frac{\int_0^T (\frac{c_1}{2}u_1^2 + \frac{c_2}{2}u^2)\,dt}{\mathcal{A}^{inf}}. \tag{19}$$

Smaller values of ACER correspond to better performances. Again, it can be seen from Table 2 that the most cost-effective strategy is to implement media campaign and rapid testing simultaneously, rather than implement them as a single interventions.

5. Conclusions

In this work, mathematical analysis of the COVID-19 transmission model with a media campaign and rapid testing has been presented. The model constructed as a system of ordinary differential equations, which separate the human population based on their health status and also their awareness. The model accommodates the media campaign to develop the community awareness on COVID-19, such that this aware population can avoid infection from COVID-19 by conducting a health protocol, such as self-isolation, social distancing, medical mask and any other intervention that can reduce the transmission rate.

From the mathematical analysis on the model, we find that the COVID-19 free equilibrium is always locally asymptotically stable whenever the basic reproduction number is smaller than one. On the other hand, the COVID-19 endemic equilibrium always exists uniquely whenever the basic reproduction number is larger than

unity. In any other case, the COVID-19 endemic equilibrium does not exist. Hence, a transcritical bifurcation occurs at basic reproduction number equal to one.

To estimate the parameter value, the model then tested with the incidence data from East Java, Indonesia. We find that the basic reproduction number in East Java is larger than one, which in this case has a high chance to reach an endemic COVID-19 situation if the intervention does not improve. To analyze the intervention strategies, we conduct our simulation as an optimal control problem. From the numerical results and cost-effectiveness analysis on the optimal control problem, we found that implementing both media campaigns and rapid testing simultaneously could give the best result compared to a single intervention. However, if the implementation should be conducted as a single intervention, then a media campaign should be implemented as a choice.

Declaration of Competing Interest

The authors declare that they have no known competing financial interests or personal relationships that could have appeared to influence the work reported in this paper.

CRediT authorship contribution statement

Dipo Aldila: Conceptualization, Methodology, Formal analysis, Software, Investigation, Validation, Writing - review & editing.

Acknowledgments

The author would like to thank the anonymous reviewer for his/her valuable comments. This research is funded by the Ministry of Research, Technology, and Higher Education / National Research and Innovation Agency (Kemenristek/BRIN) of the Republic of Indonesia with PUPT research grant scheme 2020 (ID Number: NKB-2803/UN2.RST/HKP.05.00/2020).

Appendix A. Proof of Theorem 1

From COVID-19 model in system (1), we have

$$\left.\frac{dS_u}{dt}\right|_{S_u=0,S_a\geq 0,E\geq 0,A\geq 0,I\geq 0,R\geq 0} = \Lambda + \alpha S_a > 0,$$
$$\left.\frac{dS_a}{dt}\right|_{S_u>0,S_a=0,E\geq 0,A\geq 0,I\geq 0,R\geq 0} = u_1 S_u > 0,$$
$$\left.\frac{dE}{dt}\right|_{S_u>0,S_a\geq 0,E=0,A\geq 0,I\geq 0,R\geq 0} = (\beta_1 S_u + \beta_2 S_a)(I+\sigma A) \geq 0,$$
$$\left.\frac{dA}{dt}\right|_{S_u>0,S_a\geq 0,E\geq 0,A=0,I\geq 0,R\geq 0} = p\delta E \geq 0,$$
$$\left.\frac{dI}{dt}\right|_{S_u>0,S_a\geq 0,E\geq 0,A\geq 0,I=0,R\geq 0} = (1-p)\delta E + (\xi+u_2)A \geq 0,$$
$$\left.\frac{dR}{dt}\right|_{S_u>0,S_a\geq 0,E\geq 0,A\geq 0,I\geq 0,R=0} = \gamma_1 A + \gamma_2 I \geq 0.$$

It can be seen from the above calculation, all the rates are non-negative on the boundary planes of the non-negative of $\mathbb{R}^6_+$. Therefore, we can conclude that all the vector field direction is inward from the boundary planes. Hence, whenever the system starts in a non-negative $\mathbb{R}^6_+$, all the solutions remain in the positive region only. Here the proof is completed. □

Appendix B. Proof of Theorem 2

Adding all equations in system (1) gives

$$\frac{dN}{dt} = \Lambda - \mu N - \phi I \leq \Lambda - \mu N.$$

Using the integrating factor technique, we have that $N(t)$ fulfill

$$0 \leq N \leq \frac{\Lambda}{\mu} + N(0)\exp(-\mu t).$$

Therefore, whenever the initial condition starts inside the region of Ω, then it will stay in this region. On the other hand, if the initial condition starts outside of Ω, then the solution will enter Ω and approach $\frac{\Lambda}{\mu}$ for $t \to \infty$. Hence, we have that for $t \to \infty$, we have $0 \leq N \leq \frac{\Lambda}{\mu}$. Hence, we have the theorem. □

Appendix C. Derivation of $\mathscr{R}_0$

We use the formula introduced by author in [30] for the derivation of the basic reproduction number ($\mathscr{R}_0$) in this article. The subsystem of model (1) which involve only infected compartment is given by

$$J = \begin{bmatrix} -\delta-\mu & \sigma S_1\beta_1 + \sigma S_2\beta_2 & S_1\beta_1 + S_1\beta_2 \\ \delta p & -\mu-\xi-\gamma_1-u_2 & 0 \\ (1-p)\delta & \xi+u_2 & -\gamma_2-\mu-\phi \end{bmatrix}.$$

Note that J can be expressed as a summation between transition Σ and transmission T matrices, where

$$\Sigma = \begin{bmatrix} -\delta-\mu & 0 & 0 \\ \delta p & -\mu-\xi-\gamma_1-u_2 & 0 \\ (1-p)\delta & \xi+u_2 & -\gamma_2-\mu-\phi \end{bmatrix},$$
$$T = \begin{bmatrix} 0 & \sigma S_1\beta_1 + \sigma S_2\beta_2 & S_1\beta_1 + S_2\beta_2 \\ 0 & 0 & 0 \\ 0 & 0 & 0 \end{bmatrix}.$$

Since T has two zero rows in the 2nd and 3rd row, the next generation matrix of system (1) is given by

$$\mathbf{K} = -\mathbf{E}'\,\mathbf{T}\,\mathbf{\Sigma}^{-1}\,\mathbf{E} = \left[\frac{\left(\sigma S_1^*\beta_1 + \sigma S_2^*\beta_2\right)\delta\, p}{(\mu+\xi+\gamma_1+u_2)(\delta+\mu)} + \frac{\left(S_1^*\beta_1 + S_2^*\beta_2\right)\delta\,(1-p(\mu+\gamma_1)+\xi+u_2)}{(\delta+\mu)(\mu+\xi+\gamma_1+u_2)(\gamma_2+\mu+\phi)}\right], \tag{C.1}$$

where $E = [1\,0\,0]$, while S_u^* and S_a^* is given in E_0. Hence, the basic reproduction number of system (1) is given by the spectral radius of $\mathbf{K}$. □

Appendix D. Proof of Lemma 1

To analyze the non-existence of positive roots of $\mathscr{P}(A)$ when $\mathscr{R}_0 < 1$, we will use approach of the sign of $\frac{\partial A}{\partial \mathscr{R}_0}$ at $A = 0$ and $\mathscr{R}_0 = 1$. Let β_1^* as the bifurcation parameter which is taken from the solution of $\mathscr{R}_0 = 1$ respect to β_1. Substituting β_1^* into a_2 and a_1 will give us a_2 and a_1 as a function of $\mathscr{R}_0$. By implicit derivation to $\mathscr{P}(A)$, we have $\frac{\partial A}{\partial \mathscr{R}_0}$ evaluated at $A = 0$ and $\mathscr{R}_0 = 1$ as follows :

$$\frac{\partial A}{\partial \mathscr{R}_0} = \frac{p\mu\,(\alpha+\mu+u_1)(\mu+\xi+\gamma_1+u_2)(\delta+\mu)}{a_1(\mathscr{R}_0)}, \tag{D.1}$$

where $a_1(\mathscr{R}_0) = k_2\beta_2^2 + k_1\beta_2$ with

$$k_2 = \delta\beta_2^2 u_1\Lambda(\delta+\mu)(\mu+\xi+\gamma_1+u_2)(\mu\, p\sigma + p\phi\,\sigma + p\sigma\,\gamma_2 + (1-p)(\mu+\gamma_1) + \xi + u_2)^2 > 0$$
$$k_1 = -p^2(\gamma_2+\mu+\phi)^2\mu\,(\mu+\xi+\gamma_1+u_2)(\delta+\mu)(\alpha+\mu+u_1) < 0.$$

Since the discriminant of $a_1(\mathscr{R}_0)$ which given by $k_1^2 - 4k_2\,0 = k_1^2 > 0$ when $\mathscr{R}_0 = 1$, then we always have that $a_1(\mathscr{R}_0)$ is always positive. Hence, we have that $\frac{\partial A}{\partial \mathscr{R}_0}$ is always positive at $A = 0, \mathscr{R}_0 = 1$. Hence, combine this results and Theorem 4, we have no positive roots of polynomial $\mathscr{P}(A)$ when $\mathscr{R}_0 < 1$. Hence, the proof is complete. □

Appendix E. Proof of Theorem (5)

Based on [46], our optimal control problem should satisfy the following conditions :

1. The solutions of system (11) which equipped with time-dependent control u_1 and u_2 is non empty.
2. Γ should be closed and convex and the state system can be written as a linear function of control variables u_1 and u_2, where the coefficients depending on state variables and time t.
3. Integrand of

$$\mathscr{L} = E + A + I + \frac{c_1}{2}u_1^2 + \frac{c_2}{2}u_2^2$$

is convex on Γ and $\mathscr{L} \geq f(u_1, u_2)$. Note that f is a continuous function and

$$\lim_{|(u_1,u_2)|\to\infty} \frac{f(u_1,u_2)}{|(u_1,u_2)|} = \infty.$$

Note that $|\cdot|$ represent the norm.

First of all, from Theorem (2), we have that $S_u(t)$, $S_a(t)$, $E(t)$, $A(t)$, $I(t)$, and $R(t)$ are bounded by Λ/μ. Hence, the solutions of system (11) is always bounded whenever u_1 and u_2 bounded in Γ. The right hand side of the time-dependent control COVID-19 model in (11) satisfies the Lipschitz condition with respect to S_u, S_a, E, A, I and R. Hence, we fulfilled (1) based on Picard-Lindelö theorem [47].

By definition, given the control set Γ, where $u_i \in [0, 1]^2$ for $i = 1, 2$, then we have Γ is closed. Using the definition of convex set (Proposition 2.4 in [48]), for any arbitrary points y and z in Γ, where $y = (y_1, y_2), z = (z_1, z_2)$, we have that

$$\zeta y_i + (1-\zeta)z_i \in [0,1]^2, \forall \zeta \in [0,1], \quad i = 1, 2.$$

Thus, $\zeta y + (1-\zeta)z \in \Gamma$ implying Γ is convex. The time-dependent control model in (11) is linear in control variables u_1 and u_2 with coefficients depending on the state variables S_u and A. Therefore, we have condition (2).

The integrand $\mathscr{L}$ is convex due to the quadratic form of u_1 and u_2. Furthermore,

$$\mathscr{L} = E + A + I + \frac{c_1}{2}u_1^2 + \frac{c_2}{2}u_2^2 \geq \frac{c_1}{2}u_1^2 + \frac{c_2}{2}u_2^2.$$

By choosing $c_3 = \min\{c_1, c_2\} > 0$, and $f(u_1, u_2) := c_3(u_1^2 + u_2^2)$, yields

$$\mathscr{L} = E + A + I + \frac{c_1}{2}u_1^2 + \frac{c_2}{2}u_2^2 \geq f(u_1, u_2).$$

It is clear that $f(u_1, u_2)$ is continuous and satisfy $\lim_{|(u_1,u_2)|\to\infty} \frac{f(u_1,u_2)}{|(u_1,u_2)|} = \infty$. Thus, condition (3) fulfilled. Based on [45,46], the proof is completed. □

Appendix F. Proof of Theorem (6)

The adjoint system in (15) is taken from the derivative of $\mathscr{H}$ respect to each state variable as follows

$$\frac{d\lambda_1}{dt} = -\frac{\partial \mathscr{H}}{\partial S_u}, \quad \frac{d\lambda_2}{dt} = -\frac{\partial \mathscr{H}}{\partial S_a}, \quad \frac{\partial\lambda_3}{\partial t} = -\frac{\partial \mathscr{H}}{\partial E},$$
$$\frac{d\lambda_4}{dt} = -\frac{\partial \mathscr{H}}{\partial A}, \quad \frac{d\lambda_5}{dt} = -\frac{\partial \mathscr{H}}{\partial I}, \quad \frac{d\lambda_6}{dt} = -\frac{\partial \mathscr{H}}{\partial R},$$

with the transversality condition

$$\lambda_1(t_f) = \lambda_2(t_f) = \lambda_3(t_f) = \lambda_4(t_f) = \lambda_5(t_f) = \lambda_6(t_f) = 0.$$

Furthermore, taking the first derivative of $\mathscr{H}$ respect to u_1 and u_2 gives

$$\frac{\partial \mathscr{H}}{\partial u_1} = c_1u_1 - S_u(\lambda_1 - \lambda_2), \qquad \frac{\partial \mathscr{H}}{\partial u_2} = c_2u_2 - A(\lambda_4 - \lambda_5).$$

Solving $\frac{\partial \mathscr{H}}{\partial u_i} = 0$ respect to $i = 1, 2$ gives

$$u_1^\dagger = \frac{S_u(\lambda_1 - \lambda_2)}{c_1}, \qquad u_2^\dagger = \frac{A(\lambda_4 - \lambda_5)}{c_2}.$$

By standard control arguments involving the lower bound $u_i^{\min} = 0$ and upper bound $u_i^{\max} = 1$, it follows that

$$u_1^* = \max\left\{0, \min\left\{1, \frac{S_u(\lambda_1 - \lambda_2)}{c_1}\right\}\right\},$$
$$u_2^* = \max\left\{0, \min\left\{1, \frac{A(\lambda_4 - \lambda_5)}{c_2}\right\}\right\}.$$

Hence, the proof is complete. □

References

[1] Li Q, Guan X, Wu P, Wang X, Zhou L, Tong Y, Ren R, Leung KS, Lau EH, Wong JY, et al. Early transmission dynamics in Wuhan, China, of novel coronavirus - infected pneumonia. New Engl J Med 2020.

[2] Worldometer. COVID-19 Coronavirus pandemic. 2020. https://www.worldometers.info/coronavirus/. (Accessed 13 July).

[3] Aldila D, Khoshnaw SH, Safitri E, Anwar YR, Bakry AR, Samiadji BM, Anugerah DA, H MFAG, Ayulani ID, Salim SN. A mathematical study on the spread of COVID-19 considering social distancing and rapid assessment. In: The case of Jakarta, Indonesia, Chaos, Solitons and Fractals; 2020. p. 110042. doi:10.1016/j.chaos.2020.110042.

[4] East java responses to COVID-19 official website. 2020. http://infocovid19.jatimprov.go.id. (Accessed 13 July).

[5] Bai Y, Yao L, Wei T, Tian F, Jin D-Y, Chen L, Wang M. Presumed asymptomatic carrier transmission of COVID-19. JAMA 2020.

[6] Lai C-C, Shih T-P, Ko W-C, Tang H-J, Hsueh PR. Severe acute respiratory syndrome coronavirus 2 (SARS-CoV-2) and corona virus disease-2019 (COVID-19): the epidemic and the challenges. Int J Antimicrob Ag 2020:105924.

[7] Control CfD. Preventio, coronavirus disease 2019 (COVID-19), national center for immunization and respiratory diseases (NCIRD). Division of Viral Diseases 2020. https://www.cdc.gov/coronavirus/2019-ncov/index.html. (Accessed 13 July 2020)

[8] Ngonghala CN, Iboi E, Eikenberry S, et al. Mathematical assessment of the impact of non-pharmaceutical interventions on curtailing the 2019 novel coronavirus. Math Biosci 2020;325:108364. doi:10.1016/j.mbs.2020.108364.

[9] Sarkar K, Khajanchi S, Nieto JJ. Modeling and forecasting the COVID-19 pandemic in india. Chaos Solitons Fractals 2020;139:110049.

[10] Aldila D, Ndii MZ, Samiadji BM. Optimal control on COVID-19 eradication program in indonesia under the effect of community awareness. Math Bios Eng 2020;17(6):6355–89.

[11] Khan MA, Atangana A. Modeling the dynamics of novel coronavirus (2019-nCov) with fractional derivative. Alex Eng J 2020. doi:10.1016/j.aej.2020.02.033.

[12] A Khan M, Atangana A, Fatmawati EA. The dynamics of COVID-19 with quarantined and isolation. Adv Differ Eqs 2020;1:435.

[13] Higazy M. Novel fractional order SIDARTHE mathematical model of COVID-19 pandemic. Chaos Solitons Fractals 2020;138:110007.

[14] Zhang Y, et al. Applicability of time fractional derivative models for simulating the dynamics and mitigation scenarios of COVID-19. Chaos Solitons Fractals 2020;138:109959.

[15] Silva RGd, et al. Forecasting Brazilian and American COVID-19 cases based on artificial intelligence coupled with climatic exogenous variables. Chaos Solitons Fractals 2020;139:110027.

[16] Singh S, Parmar KS, Kumar J, Makkhan SJS. Development of new hybrid model of discrete wavelet decomposition and autoregressive integrated moving average (ARIMA) models in application to one month forecast the casualties cases of COVID-19. Chaos Solitons Fractals 2020;135:109866.

[17] He S, Tang S, Rong L. A discrete stochastic model of the COVID-19 outbreak: forecast and control. Math Biosc Eng 2020;17(4):2792–804.

[18] German R., Djanatliev A., Maile L., Bazan P., Hackstein H.. Modeling exit strategies from COVID-19 lockdown with a focus on antibody tests. 2020, 10.1101/2020.04.14.20063750.

[19] Yang J, Wang G, Zhang S. Impact of household quarantine on SARS-CoV-2 infection in mainland China: a mean-field modelling approach. Math Biosc Eng 2020;17(5):4500–12.

[20] Atangana A, Araz SI. Mathematical model of COVID-19 spread in Turkey and South Africa. Theory Methods Appl 2020. doi:10.1101/2020.05.08.20095588.

[21] Ndii M, Hadisoemarto P, Agustian D, Supriatna A. An analysis of COVID-19 transmission in Indonesia and Saudi Arabia. Commun Biomath Sci 2020;3(1).

[22] Feng Z, Velasco-Hernndez JX. Competitive exclusion in a vector-host model for the dengue fever. J Math Biol 1997;35(5):523–44. doi:10.1007/s002850050064.

[23] Ferguson NM, Laydon D, Nedjati-Gilani G, Imai N, Ainslie K, Baguelin M, Bhatia S, Boonyasiri A, Cucunuba Z, Cuomo-Dannenburg G, et al. Impact of non-pharmaceutical interventions (NPIs) to reduce COVID-19 mortality and healthcare demand Imperial college COVID-19 response team, London, vol. 16; 2020.

[24] Li Q, Guan X, Wu P, Wang X, Zhou L, Tong Y, Ren R, Leung KS, Lau EH, Wong JY, et al. Early transmission dynamics in Wuhan, China, of novel coronavirus infected pneumonia. New Engl. J. Med. 2020.
[25] Lauer SA, Grantz KH, Bi Q, Jones FK, Zheng Q, Meredith HR, et al. The incubation period of coronavirus disease 2019 (COVID-19) from publicly reported confirmed cases: estimation and application. Ann. Int. Med. 2020.
[26] del Rio C, Malani PN. COVID-19 New insights on a rapidly changing epidemic. JAMA 2020.
[27] Anderson RM, Heesterbeek H, Klinkenberg D, Hollingsworth TD. How will country-based mitigation measures influence the course of the COVID-19 epidemic? Lancet 2020;395(10228):931–4.
[28] World Health Organization. Coronavirus disease 2019 (COVID-19): situation report, 46, WHO. 2020.
[29] Tang B, Wang X, Li Q, Bragazzi NL, Tang S, Xiao Y, Wu J. Estimation of the transmission risk of the 2019-nCoV and its implication for public health interventions. J Clin Med 2020;9(2):462.
[30] Diekmann O, Heesterbeek JA, Roberts MG. The construction of next-generation matrices for compartmental epidemic models. J R Soc Interface 2010;7(47):873–85. doi:10.1098/rsif.2009.0386.
[31] Driessche PV, Watmough J. Reproduction numbers and sub-threshold endemic equilibria for compartmental models of disease transmission. Math Biosci 2002;180:29–48.
[32] Diekmann O, Heesterbeek JA, Metz JA. On the definition and the computation of the basic reproduction ratio R0 in models for infectious diseases in heterogeneous populations. J Math Biol 1990;28(4):365–82. doi:10.1007/BF00178324.
[33] Wijaya KP, Chavez JP, Aldila D. An epidemic model highlighting humane social awareness and vector-host lifespan ratio variation. Commun Nonlinear Sci Numer Simulat 2020. doi:10.1016/j.cnsns.2020.105389.
[34] Handari BD, Vitra F, Ahya R, Aldila D. Optimal control in a malaria model: intervention of fumigation and bed nets. Adv Differ Eqs 2019;2019(1):497.
[35] Aldila D, Götz T, Soewono E. An optimal control problem arising from a dengue disease transmission model. Math Biosci 2013;242(1):9–16. doi:10.1016/j.mbs.2012.11.014.
[36] Garba SM, Gumel AB, Abu Bakar MR. Backward bifurcations in dengue transmission dynamics. Mathematical biosciences 2008;215(1):11–25. doi:10.1016/j.mbs.2008.05.002. PMID: 18573507
[37] Reluga TC, Medlock J, Perelson AS. Backward bifurcations and multiple equilibria in epidemic models with structured immunity. Journal of theoretical biology 2008;252(1):155–65. doi:10.1016/j.jtbi.2008.01.014. PMID: 18325538
[38] Knipl DH, Ro st G. Backward bifurcation in SIVS model with immigration of non-infectives. BIOMATH 2014;2(2):1–14. doi:10.11145/j.biomath.2013.12.051.
[39] Chitnis N, Hyman JM, Cushing JM. Determining important parameters in the spread of malaria through the sensitivity analysis of a mathematical model. Bull Math Biol 2008;70(5):1272–96. doi:10.1007/s11538-008-9299-0.
[40] Agusto FB, ELmojtaba IM. Optimal control and cost-effective analysis of malaria/visceral leishmaniasis co-infection. PLoS One 2017;12(2):e0171102. doi:10.1371/journal.pone.0171102. Published 2017 Feb 6
[41] Kumar A, Srivastava PK, Dong Y, Takeuchi Y. Optimal control of infectious disease: information-induced vaccination and limited treatment. Physica A 2020;542:123196.
[42] Joshi HR, Lenhart S, Hota S, Agusto F. Optimal control of an SIR model with changing behavior through an education campaign, electron. J Differ Eqs 2015;2015(50):1–14.
[43] Aldila D, Padma H, Khotimah K, Desjwiandra B, Tasman H. Analyzing the MERS disease control strategy through an optimal control problem. Int J Appl Math Comput Sci 2018;28(1):169–84.
[44] Aldila D. Cost-effectiveness and backward bifurcation analysis on COVID-19 transmission model considering direct and indirect transmission. Commun Math BiolNeurosci 2020;49:1–28.
[45] Gaff H, Schaefer E. Optimal control applied to vaccination and treatment strategies for various epidemiological models. Math Biosci Eng 2009;6(3):469–92.
[46] Fleming WH, Rishel RW. Deterministic and stochastic optimal control, vol. 1. New York: Springer; 1975.
[47] Coddington EA, Levinson N. Theory of ordinary differential equations. Tata McGraw-Hill Education; 1955.
[48] Romero-Leiton JP, Montoya-Aguilar JM, Ibargen-Mondragn E. An optimal control problem applied to malaria disease in Colombia. Appl Math Sci 2018;12(6):279–92. doi:10.12988/ams.2018.819.
[49] Pontryagin L.S., Boltyanskii V.G., Gamkrelidze R.V., Mishchenko E.F.. The mathematical theory of optimal processes. 1962.
[50] Lenhart S, Workman JT. Optimal control applied to biological models. CRC Press; 2007.